PERFORMANCE OF AMMONIA-FIRED GAS-TURBINE COMBUSTORS

by

D. T. Pratt

Report No. TS-67-5
Contract DA-04-200-AMC-791(x)

August 1967

COLLEGE OF ENGINEERING
UNIVERSITY OF CALIFORNIA, Berkeley

35

UNIVERSITY OF CALIFORNIA
Department of Mechanical Engineering
Thermal Systems Division

PERFORMANCE OF AMMONIA-FIRED GAS-TURBINE COMBUSTORS

by

D. T. Pratt

Technical Report No. 9

Under Contract
DA-04-200-AMC-791(x) Ammonia Fuel
Army Materiel Command
R & D Directorate
Chemistry and Materials Branch

Project Director
E. S. Starkman

August, 1967

SUMMARY

A theoretical and experimental program was undertaken to investigate scaling and combustion in gaseous ammonia-fired gas turbine combustors.

Theoretical analysis of performance and scale test data previously performed by the Solar Company strongly indicates that the final size chosen for an operating gas turbine is performance-limited almost equally by chemical reaction kinetics (residence time) and by turbulent diffusion or mixing processes (velocity or Reynolds number). It was found that the Solar blowout data may be correlated with a pressure exponent or "effective reaction order" of 1.18.

Experimentally, a 3/5-scale combustor was fabricated, geometrically similar to the final configuration adopted by Solar, and a performance map was obtained at the same operating conditions as the Solar prototype combustor. Results confirmed that the small-diameter combustor is chemically rate-limited at pressures very slightly less than the minimum reported in the Solar data, and becomes limited almost equally by chemistry and mixing at higher pressures.

The fundamental problem with utilizing gaseous ammonia as a turbine fuel is certainly the relatively slow (compared to hydrocarbon fuels) chemical reaction between ammonia and air. As air flow is reduced, to allow sufficient residence time for the reaction to progress, diminished Reynolds number effects lead to less efficient mixing. This in turn leads to decreased combustion efficiency. The only apparent solutions (apart from chemical enrichment by cracking or use of additives) are to use a smaller fuel nozzle orifice to create a more vigorous fuel jet in the primary zone, and to use two or more combustors in parallel rather than build a single larger combustor. While both of these solutions have been widely applied in hydrocarbon-fueled gas turbine technology, the problems in increased bulk and frontal area of the combustor are magnified.

TABLE OF CONTENTS

LIST OF FIGURES

I. INTRODUCTION

This is the final report on research undertaken at the University of California at Berkeley to investigate properties of ammonia as a fuel for internal combustion engines, under contract number DA-04-200-AMC-791(x) of the Army Materiel Command. This report is concerned with problems of aerodynamical and chemical processes encountered in designing ammonia-fired gas turbine combustion chambers.

In report number DA-0990-AMC dated 23 July, 1967, "Development of an Ammonia-Burning Gas Turbine Engine," (Reference 1) the Solar company reported difficulties in obtaining scaling laws required to predict performance of scaled ammonia-fired combustors from performance data obtained from a prototype combustor. Specifically, it was stated that "at present, it is not known whether velocity or residence time is the major influence." (p. 30, Reference 1). The present investigation of this problem was undertaken along two lines: first, to perform an analytical investigation of the results presented by Solar, and second, to build a reduced-scale model of the final configuration adopted by Solar, obtain performance data from it and determine whether or not the theoretical conclusions concerning the model laws were supported.

II. THEORETICAL ANALYSIS

1. Background. Model scaling laws have been only moderately successful for liquid hydrocarbon-fueled combustors, due to such difficult-to-scale phenomena as carbon deposition and fuel atomization and distribution. However, gas-fired combustors, which lack these problems, are somewhat more amenable to theoretical analysis. The final combustor configuration adopted by Solar (Figure 1) is

especially "clean" from this standpoint; the very constrictive primary and secondary air admission holes (necessitated by the relatively low approach velocities) insure that the fraction of air in the primary zone is virtually constant and predictable from design area ratios, and the open-tube fuel nozzle (Figure 2) simplifies or eliminates nozzle-jet scaling problems.

2. Fundamental Modeling Considerations. In Reference 2, Spalding discussed the general problem of modeling in combustion systems. He pointed out that the strict requirements of similarity are so numerous as to be impossible of obtaining. The limited success of modeling lies in the "art", that is, in determining which dimensionless groups can be ignored.

Fifteen years of work by many investigators showed that in liquid and gas-fired hydrocarbon-fueled combustors, similarity could be adequately modeled by Reynolds number and a "chemical loading group", or ratio of residence time to some measure of characteristic reaction time. Strict application of these criteria led to the formulation of "p-d" scaling, in which a geometrically similar model and prototype would be effectively similar if fired with the same fuel at the same inlet temperature and equivalence ratio, and (if the chemical reaction is assumed to be a second-order reaction overall) the same primary zone velocity, and pressures in inverse ratio to the linear diameter or characteristic dimensions. Scaling on the basis of "p-d" has been very successfully applied to afterburners and ramjet combustors, but somewhat less so to gas-turbine combustors. (2,3,4,5).

A description of the role of Reynolds number and chemical loading in hydrocarbon-fueled gas turbine combustors was given by Herbert (3,6), in which he concluded that for model and prototype with the same fuel, equivalence ratio and inlet temperature, combustion efficiencies and blowout conditions could be correlated by

$$I(Re)^b = \text{const.}$$

where I is the chemical loading group,

$$I = \dot{m}/d^3p^2 \propto u/pd$$

and Re the Reynolds number,

$$Re = udp/\mu \propto udp$$

and b is an experimentally determined constant.

Therefore

$$I(Re)^b \propto \frac{u}{pd}(pdu)^b = u^{b+1}(pd)^{b-1},$$

and since the absolute value of the exponent or the entire group is of no consequence, it is permissible to take the "b+1"-th root of the expression:

$$u(pd)^{\frac{b-1}{b+1}} = \text{const.}'$$

Denoting $\frac{b-1}{b+1} \equiv c - 1$,

the correlating group takes the form

$$\frac{u}{pd}(pd)^c = \text{const.}'' \qquad (1)$$

with no loss of generality, where the exponent c reflects the influence of mixing processes on the chemical loading: $b = c = 0$ implies that the reaction is entirely chemically limited. Herbert (3) gives $b = c = 1$ as an upper limit. (Presumably, if mixing processes were limiting, $b \to \infty$ and $c = 2$. However, this regime is not of much practical interest because the flow rates at which entirely aerodynamic blowoff occurs are usually greater than those encountered in practical combustor technology.) Therefore it is apparent that this correlation is applicable only to high-output systems in which chemical loading plays an essential role, modified by Reynolds number effects. Herbert pointed out that for Longwell's

stirred reactor (7), c = 0.2, while for some practical turbojet combustors, c = 0.5. In theory, c should not be expected to be constant over a wide range of operating conditions for any given reactor (the analysis of Reference 8 in fact shows this variation), but Herbert concluded that, for the data at hand, Reynolds number was always sufficiently high that the nature of the influence of mixing on chemical loading was more or less constant.

Alternately, the effect of the exponent b or c is often expressed as the "effective reaction order" for the overall chemical reaction, defined as follows:

Rewriting equation (1) in terms of the mass or molar flow rate $\dot{m}$,

$$\frac{u}{pd}(pd)^c = \frac{u}{(pd)^{1-c}} \propto \frac{\dot{m}}{pd^2(pd)^{1-c}} = \frac{\dot{m}}{d^{3-c}p^{2-c}} = \text{const.}'''$$

and if the primary zone volume is substituted in the expression in place of the combustor diameter,

$$d \propto V^{1/3} \rightarrow \frac{\dot{m}}{d^{3-c}p^{2-c}} \propto \frac{\dot{m}}{V^{1-c/3}p^{2-c}} = \text{const.}''''$$

Identifying the exponents of V and p as m and n respectively,

$$\frac{\dot{m}}{V^m p^n} = \text{const.}''''' \qquad (2)$$

where b, c, m and n correspond as follows:

b	c = 2b/b+1	m = b+c/c(b+1)	n = 2/b+1
0	0	1	2
1	1	2/3	1
∞	2	1/3	0

and n is called the "pressure exponent" or "effective reaction order."

All of the above theory and experiment was carried out specifically for hydrocarbon-fueled combustors, and should not be expected to hold rigorously for ammonia-fueled combustors, since both laminar and turbulent flame speeds for ammonia have long been known to be much smaller than for hydrocarbons, (9,10), indicating a significantly slower chemical reaction. In particular, it is to be expected that slower reactions would require lower combustor velocities and hence lower Reynolds numbers, which in turn suggests that the exponent c might be strongly variable for ammonia-air combustion systems over a wide range of operating conditions.

3. Application to Solar's Scaling Tests. To evaluate scale effects, Solar tested 4 combustors of liner diameter 5, 6, 7, and 8 inches (Figure 9 of Reference 1), all apparently housed in an 8.5-inch outer casing. Their performance results are summarized in Figure 10 of Reference 1. From these results, 6.75 inches was chosen as optimum liner diameter. Solar reported that "There is no obvious explanation of the relative vertical shifts of the stability loops or of the reduced loop obtained with the 8-inch diameter combustor."

Since inlet pressure and temperature are fixed, for this data,

$$Re \propto ud$$

and

$$I \propto u/d = (\text{mean residence time})^{-1}$$

The latter expression holds only if the fuel-air equivalence ratio and combustion efficiencies are constant. If the "nose" of each stability loop is regarded as the data point for comparison, then the primary zone fuel-air ratio may be assumed to be near the stoichiometric value, or an equivalence ratio of unity (6). However, no data are given concerning combustion efficiencies.

The following values are readily obtained from Figure 10 of Reference 1:

d (in)	u_{max} (fps)	ud(∝ Re)	d/u (= Residence time)
5	4.2	21.1	1.19
6	6.8	40.8	0.88
7	7.5	52.5	0.93
8	6.5	52.0	1.23

These values are plotted in Figure 7.

In attempting to draw conclusions from Figure 7 in the light of the modeling relations (eqn. 1), it must be emphasized that the family of Solar combustors are <u>not</u> geometrically similar, since the outer housing is the same size in every case; only the liners are geometrically similar. Still, the product ud is proportional to Reynolds number, and d/u is proportional to residence time in the primary zone, although not necessarily proportional to the chemical loading I.

Figure 7 shows that the primary zone velocity is maximized for this family of combustors for a diameter of about 6.75 inches. Presumably, the final choice of diameter was made on this basis (although Solar comments that "the diameter was made as large as possible without redesign of the turbine entry scroll.") The residence time at maximum blowout conditions is minimized for a diameter of about 6.25 inches. The Reynolds number initially increases with diameter, and becomes constant for the 7 and 8-inch liners.

The latter fact suggests that mixing processes are limiting the performance of the 7 and 8-inch combustors. The fact that lower Reynolds numbers are achieved in the smaller liners at blowout velocity infers that other mechanisms are controlling. It is assumed, since the ammonia-air reaction is known to be a relatively slow one, that blowout is caused by chemical kinetics limitations. As mentioned above, the absence of combustion efficiency data

precludes a direct conclusion concerning the chemical loading, but there is nothing apparent in the data to contradict this conclusion.

It would seem, then, that for the inlet temperature and pressure at which the tests were made, a liner smaller than about 6.5 inches is primarily chemically rate-limited at maximum blowout velocity. For larger diameters, the blowout velocity is primarily diffusion-limited. While the design details of the final liner configuration are different from those used in the series of model tests, it is probable that chemical kinetics and turbulent mixing processes are of approximately equal importance, at least for inlet pressures and temperatures near those of the scaling tests: P = 26 psia and T = 370°F. If this is the case, one would expect a value of approximately unity for the exponent b in the correlating group $I(Re)^b$ = const.*

A plausible explanation for the vertical shift of the maximum blowout points is as follows: The upward shift from 5-in to 6-in could be simply due to the fact that the increased liner frontal area, with the housing area constant, entrained more primary air. Thus an equivalence ratio of unity in the primary zone would correspond to an increased overall equivalence ratio. The downward shift from 6" to 7" to 8" is somewhat more puzzling. However, if the mixing processes are becoming less efficient with increased diameter (i.e., unable to properly mix cold reactants and hot products, causing extinction), more of the primary air would pass through unreacted. Thus an increase of primary air/fuel ratio (required to achieve an equivalence ratio of unity in the fraction of air that reacts) would lead to a reduced overall equivalence ratio. This behavior

---

* b = 1 in effect gives equal weight to chemical and aerodynamical processes. The difference between this and "p-d" scaling is that b = 1 requires only the product I(Re) = const., while "p-d" scaling requires $I = \text{const.}_1$ and $Re = \text{const.}_2$ independently.

is consistent with known effects of increasing liner diameter (with fixed housing diameter) on jet penetration and mixing in parallel-walled combustors with flush secondary air holes (11).

4. Chemical Kinetics for Homogeneous Gas-phase Chemical Reactions. Assuming complete homogeneity in the primary reaction zone and second-order chemical reaction, the theoretical dependence of chemical loading on equivalence ratio ϕ, inlet conditions and oxygen (or fuel) consumption efficiency ε is readily obtained from stoichiometry (for the particular reaction of interest) and basic definitions of reaction rates in a perfect-stirred reactor (7):

$$I \equiv \frac{N_A}{VP^2} = \frac{k}{(RT)^2} \cdot \frac{42.84\ (1 - y\varepsilon)(\phi - y\varepsilon)}{y\varepsilon[4\phi + 14.28 + y\varepsilon]^2}, \quad \left[\frac{\text{g mol}}{\text{cc-sec-atm}^2}\right]$$

$$\text{where } y = \begin{cases} \phi \text{ if } \phi < 1 \\ 1 \text{ if } \phi \geq 1 \end{cases} \qquad \text{and } k = 10^{14.61} \exp\left(\frac{-38,7000}{RT}\right), \quad \left[\frac{\text{cc}}{\text{g mol-sec}}\right]$$

from Reference 12, and T is the actual reaction zone temperature, obtained from the energy equation with equivalence ratio, fuel consumption efficiency and inlet T and P.

In practice, the loading I can be obtained experimentally, the reactant consumption efficiency ε calculated from measured temperature-rise combustion efficiency η, equivalence ratio, and the assumption that incomplete combustion results in the presence of unburned fuel alone (an assumption strongly supported by the odor of ammonia in the exhaust quenching water). The above equation can then be solved for an effective rate constant k_{eff} which can then be compared with the value from Reference 12 also cited above. The ratio k_{eff}/k_{theo} then serves as an index of how close the blowout point is to being chemically limited.

III. EQUIPMENT

1. Combustor. The combustor liner was a 3/5-scale model of the final design adopted by Solar, as shown in Figures 1 and 2. The housing was a 5.1 inch I.D. Pyrex "Double-Tough" pipe, 16 inches long (Figure 4). To avoid penetrating the wall of the Pyrex housing, the fuel was introduced through a 5/16 inch Inconel nozzle shown in Figure 2. Ignition was accomplished by a spark-ignited propane torch. The propane was introduced to the primary zone of the combustor through an 8 mm quartz tube on the axial centerline of the assembly, the tube terminating just inside the upstream end of the liner, facing the fuel nozzle opening. The ignition spark was supplied from a 120/12,000 volt AC transformer, with the electrode passing down the center of the 8 mm quartz propane tube. The spark gap was about 1/8 inch, from the electrode to the inner wall of the grounded liner. Propane and ignition spark were used only briefly to ignite the ammonia-air mixture. No data were taken with propane flow and/or spark energized.

2. Fuel Supply and Metering. The ammonia was vaporized in a steam-water bath (Figures 3 and 6), the rate of vaporization and hence the vaporization pressure being controlled by the rate of heat supply and fuel flow. Metering was accomplished by an air-calibrated Fischer-Porter "Stable-Vis" rotameter immediately downstream of a pressure regulating valve (Figure 3). The rotameter float was chosen for its insensitivity to viscosity changes, hence only density corrections were required to the air-calibrated apparent flow rate. Density was determined from the vaporization and delivery pressures of the pressure regulator, a pressure-enthalpy diagram for ammonia, and the assumption of an equal-enthalpy throttling process across the regulator. (This calculation was performed in the data reduction program.) A solenoid valve was installed in the fuel line to permit quick shutdown, and a temperature-sensor in the exhaust line was preset to actuate

the valve at 325 F in the event of failure of the cooling water system. Coarse control was achieved by the pressure regulator setting, and fine control by a needle valve immediately prior to entry into the combustor housing.

3. Air Supply and Metering. Air was obtained from house air supply, fed by a single compressor which supplied 415 SCFM at 100 psig. After regulation to desired pressure, the air passed through a 0.6 inch diameter sharp-edged orifice in a 2.5 foot section of 2 inch pipe, then through a positive displacement meter (which could be bypassed for high flow rates), through a fine and coarse control valve, and finally into a 5-foot long approach section of 5 inch steel pipe containing six 220 volt 6 KW air heaters (calrod units) extending 4 feet into the approach section and covered with 1 inch of "Kaolin" insulation. The six heaters were individually switched, and one was connected to a "Variac" transformer to allow fine temperature control for fixed air mass-flow rates. A pitot-tube rake assumbly of three tubes, located on area-centerlines of three equal areas, was installed at the exit end of the air approach section.

4. Instrumentation. All temperatures were measured with Chromel-Alumel thermocouples, of simple exposed-junction type, except for the three hot gas measuring thermocouples, numbers 3, 4, and 5. These three were radiation-shielded by an open tee-shield of 1/4-inch Inconel tube, so that the junction did not "see" the cold walls of the exhaust gas section. Thermocouple output emf's were read from a Wheatstone-bridge null-balance potentiometer to the nearest one-hundredth of a millivolt.

All static pressures were measured with standard process-grade Bourdon pressure gages; pressure differentials were measured by U-tube manometers with fluids appropriate to the pressure differential level.

IV. EXPERIMENTAL PROCEDURE

Blowout data were obtained by first fixing the inlet air mass flow rate and temperature and then adjusting the ammonia flow rate until either rich or lean blowout occurred. The pressure level was then readjusted to the desired value while burning just below blowout conditions. This procedure was repeated typically three or four times until a reproducible stable burning configuration was obtained with the desired values of inlet conditions and mass flow rate, such that a small increase in air flow rate would cause blowout. In many cases, blowout would not occur for as long as two minutes after adjustment from stable burning, a time lag being required for low frequency pulsations to grow in amplitude until the flame was finally extinguished.

Maximum blowout data were obtained in the same manner, except that the air flow rate was advanced on each trial until there was no distinction between rich and lean blowout; that is, a single blowout point was obtained for the fixed inlet mass flow rate of air.

For each stable blowout point, temperatures were monitored until no time variations occurred, at which time all thermocouple outputs, pressures, and mass flow rates of air, fuel, cooling water and condensate were recorded. (Measurements of the latter two quantities, along with their respective temperatures and pressures, were used to check the observed gas temperatures by performing an energy balance on the system.)

V. EXPERIMENTAL RESULTS

1. Rich and lean blowout data were obtained for the 3/5-scale combustor at the same inlet temperature and pressure as the Solar prototype operating at 25% load. Results are presented as overall equivalence ratio vs. chemical loading (Figure 8). The stability loop obtained fits slightly within the Solar data loop. The maximum loading was .60, compared to 0.72 for the Solar combustor. The data obtained give the following ratios at maximum blowout: $\frac{Re_2}{Re_1} = 0.29$ and $\frac{I_2}{I_1} = .83$, where 2 denotes the smaller combustor. The maximum blowout velocities were $V_1 = 11.4$ fps and $V_2 = 5.5$ fps.

All blowout points were characterized by low-frequency pulsations (1/2 to 1 Hz), most strongly with lean blowout conditions, which made accurate determination of blowout limits difficult. The data presented in Figure 4 represent stable burning, hence may be considered to be conservative. This observation is strengthened by the fact that the maximum blowout combustion efficiency was greater for the smaller combustor than for the prototype. Other investigators also reported low frequency pulsations at some lean blowout conditions (1,10). The presence of low-frequency acoustic instabilities in three independent sets of data indicates an important problem area in which little work has been done (13). There is reason to suspect that the solution to this problem lies in redesign of the fuel nozzle.

2. To investigate further the relative influences of Reynolds number and chemical loading, a series of tests was made with a constant inlet temperature of 122 $\pm$ 2 degrees F, varying the pressure and obtaining values of chemical loading, Reynolds number, equivalence ratio and combustion efficiency at maximum blowout conditions. The results of these tests, as well as the same data inferred from the Solar data, is presented as Figure 9, for which the slope of the best-fit line through the data points is the exponent b referred to earlier.

The Solar data, which represents a wide range of inlet temperatures and pressures, are fit well by a value of b = 0.7, which corresponds to an effective reaction order n = 1.18. For the smaller combustor, a distinct change of slope is evident, decreasing from b ≈ 1 (n = 1) to b = 0.7 (n = 1.18) as the pressure was decreased from 28.4 psia to 10.5 psia, clearly indicating a transition from chemical and mixing limiting to purely chemical limiting at sub-atmospheric pressures. Fuel mass flow limitations prevented obtaining data points for higher Reynolds numbers (and pressures) at stoichiometric equivalence ratio.

3. Combustion efficiencies for all data points collected are plotted vs. chemical loading in Figure 10.

4. Effective rate constants were calculated from collected data and the ratio of effective rate constant to theoretical rate constant at measured temperature (with values from Reference 12) are plotted versus chemical loading in Figure 11.

VI. ANALYSIS OF RESULTS

1. Solar Performance Data. Performance of the 6.75-inch diameter liner designed by Solar was presented as primary zone velocity vs. temperature rise (Figures 13 through 22 of Reference 1), from which chemical loading I and Reynolds number at maximum blowout conditions were readily obtained. These values are plotted in Figure 9, from which the slope of the log-log plot gives a value of 0.7 for the exponent b of equation (1), and hence a value of c = 2b/b+1 = 0.83 and effective reaction order n = 2 - c = 1.18, which implies that chemical kinetics and mixing effects are of about equal importance in determining maximum blowout. Since values of c of 0.5 to 0.7 have been reported for non-premixed hydrocarbon-fueled combustors (3,8), this suggests that there is perhaps room for improvement for the effectiveness of the mixing processes in the Solar designed combustor. The fact

that lower flame speeds require lower velocities and hence less efficient mixing processes is reflected in Solar's design by the fact that the ratio of secondary air hole area to housing cross-sectional area is only 0.114, compared to a value of typically 0.8 for a hydrocarbon-fueled combustor. The result is that the pressure loss is still about of the same order of magnitude as with a hydrocarbon combustor; if it were necessary to use this liner for burning hydrocarbon fuels, the pressure loss would be unacceptably high.

2. Combustion Efficiency. Figure 10 shows a decrease in combustion efficiency with increased chemical loading, as should be expected. The highest combustion efficiency recorded was 83% at very low loading. Apparently, the mixing processes are not efficient enough to produce high combustion efficiencies. These values were influenced by non-uniform temperature gradients in the outlet station, where the three temperatures recorded at the same axial station showed differences of as much as 100°F in the cross-sectional outlet stream. Typically, the station at 12 o'clock (facing downstream) was 75 to 100°F cooler than the stations at 8 o'clock and 5 o'clock, which were usually within 25°F of each other. Thermocouple error was suspected, but interchanging thermocouples confirmed that the temperature differences were real; the upper portion of the exhaust stream was consistently cooler than the lower part in every run. However, this could not have affected values of combustion efficiency by more than $\pm$ 5%. Since the surface-to-volume ratio of the model was 5/3 that of the Solar combustor, it would be expected that flame quenching at the liner walls would lead to a lower combustion efficiency. On the other hand, the smaller combustor would be expected to have somewhat more efficient mixing processes, due to the smaller scale of turbulence and the reduced radius of the liner into which mixing jets must penetrate. In fact, these scale effects apparently did not affect the results greatly, as Solar reported similar values of combustion efficiencies

for the same inlet conditions. However, from the Solar and Allison reports it appears that combustion efficiencies increased markedly with increased inlet temperature, values in excess of 100% having been reported by both groups (1,10).

3. Effective Reaction Order. At present, the chemical reaction of ammonia with oxygen in the presence of nitrogen is thought to be an overall second-order reaction (5). Therefore, the effective reaction order n is a direct measure of the relative influence of chemical and aerodynamical processes in determining the efficiency of reaction completion, as explained earlier. The Solar data is shown in Figure 9 to correlate very well with an effective reaction order of 1.18, which indicates about equal influences of chemical and aerodynamic processes at blowout conditions. The model data shows this trend at atmospheric pressure and higher, but shows a rapid transition to almost completely chemical control at even slightly sub-atmospheric pressures.

4. Effective Rate Constant. It is apparent from Figure 11 that, for a given loading, the effective rate constant is nearer the theoretical chemical value for small equivalence ratios. This is because the abundance of oxidizer makes intimate contact of fuel and oxidizer more likely, and less fuel passes through the combustor unreacted. While the results are considerably scattered, which in part reflects the many assumptions required to calculate them, the overall trend is of great importance: as loading increases, the rate constant gets closer to the theoretical or homogeneous mixing value.

VII. CONCLUSIONS

1. Scaling. Both scaling tests conducted were less than perfect: Solar's lacked geometric similarity, and the present tests were not performed on the same test rig as the Solar tests, so that only tentative conclusions can be drawn:

A. For diameter scaling, the model can be expected to have the same stability limits as the prototype when both are operating at the same inlet temperature, pressure and equivalence ratio, and at the same value of chemical loading I.

B. For a given combustor, with varying inlet pressure and temperature, but with a fixed equivalence ratio, flame extinction or blowout will occur at the same value of $I(Re)^{0.7}$.

2. Combustion Efficiency. Values of combustion efficiencies measured, at air inlet conditions of 122°F and 16.2 psia, even for low loadings (i.e., far from blowout condition), were unacceptably low for gas turbine cycle operation. This, with the fact that aerodynamic processes were observed to play a co-equal role with chemical kinetics in limiting operation of the combustor for all inlet temperatures and pressures, indicates a major problem in mixing fuel, air and hot products in the primary zone. These mixing processes are obviously much less effective than in a hydrocarbon-fueled combustor, and will probably require some moderately extensive development to become optimized. Because of the much lower flame speed of the ammonia-air reaction (compared to hydrocarbons), new and unique techniques may be required to achieve this mixing.

VIII. NOMENCLATURE

b	Influence exponent, defined in Section II.2.
c	$2b/b + 1$.
d	Diameter.
I	Chemical loading. $I \equiv N_A/VP^2$ (g mol/cc-sec-atm^2).
k	Chemical-kinetic rate constant, defined in Section II.4.
$\dot{m}$	Mass flow rate.
N_A	Molar flow rate of air, gram-moles/sec.
n	Effective reaction order or pressure exponent, defined in Section II.2. $n = 2/b + 1$.
P	Absolute pressure.
Re	Reynolds Number. $Re \equiv \frac{udp}{\mu}$.
T	Temperature.
u	Velocity.
V	Volume of primary reaction zone.
ϵ	Reactant consumption efficiency. ($\epsilon = 1$ implies reaction has gone to completion.)
η	Combustion efficiency, defined as ratio actual temperature increase to maximum theoretical temperature increase.
ϕ	Fuel-air equivalence ratio, defined as ratio of actual fuel-air ratio to stoichiometric fuel-air ratio.
μ	Viscosity.

REFERENCES

1. "Development of an Ammonia-Burning Gas Turbine Engine," Report No. DA-44-009-AMC, Solar, Inc., July 1965.

2. Spalding, D. B., "The Art of Partial Modeling," 9th Symposium on Combustion, Academic Press, 1963.

3. Herbert, M. V., "Aerodynamic Influences on Flame Stability," Progress in Combustion Science and Technology, Vol. I, Pergamon Press, 1960.

4. Stewart, D. G. and Quigg, G. C., "Similarity and Scale Effects in Ramjet Combustors," 9th Symposium on Combustion, Academic Press, 1963.

5. Lefebvre, A. H. and Halls, G. A., "Some Experiences in Combustion Scaling," Advanced Aero Engine Testing, Pergamon Press, 1959.

6. Herbert, M. V., "A Theoretical Analysis of Reaction Rate Controlled Systems - Part I," AGARD Combustion Researches and Reviews 1957, Butterworths Scientific Publications, 1957.

7. Longwell, J. P. and Weiss, M. A., "High Temperature Reaction Rates in Hydrocarbon Combustion," Journal of Industrial and Engineering Chemistry, Vol. 47, No. 8, 1955.

8. Childs, J. H. and Graves, C. C., "Correlation of Turbine-Engine Combustion Efficiency with Theoretical Equations," 6th Symposium on Combustion, Reinhold Publishing Co., 1957.

9. Samuelson, G. S., "Flame Propagation Rates in the Combustion of Ammonia," Report No. TS-65-4 (DA-04-200-AMC-791(x)), University of California, Berkeley, 1965.

10. Verkamp, F. J., Hardin, M. C. and Williams, J. R., "Ammonia Combustion Properties and Performance in Gas Turbine Burners," 11th Symposium on Combustion, The Combustion Institute, 1967.

11. Graves, C. C. and Grobman, J. S., "Theoretical Analysis of Pressure Loss and Airflow Distribution in Tubular Parallel-Walled Turbojet Combustors," NACA Report 1373, 1958.

12. Sawyer, R. F., "The Homogeneous Gas Phase Kinetics of Reaction Rates in the Hydrazine-Nitrogen Tetroxide Propellant System," Ph.D. Thesis, Princeton University, 1965.

13. [illegible]ng, M. W., "A Non-acoustic Theory of Oscillations in Pressure-jet Oil-fired Combustion Chambers," 7th Symposium on Combustion, Butterworths Scientific Publications, 1959.

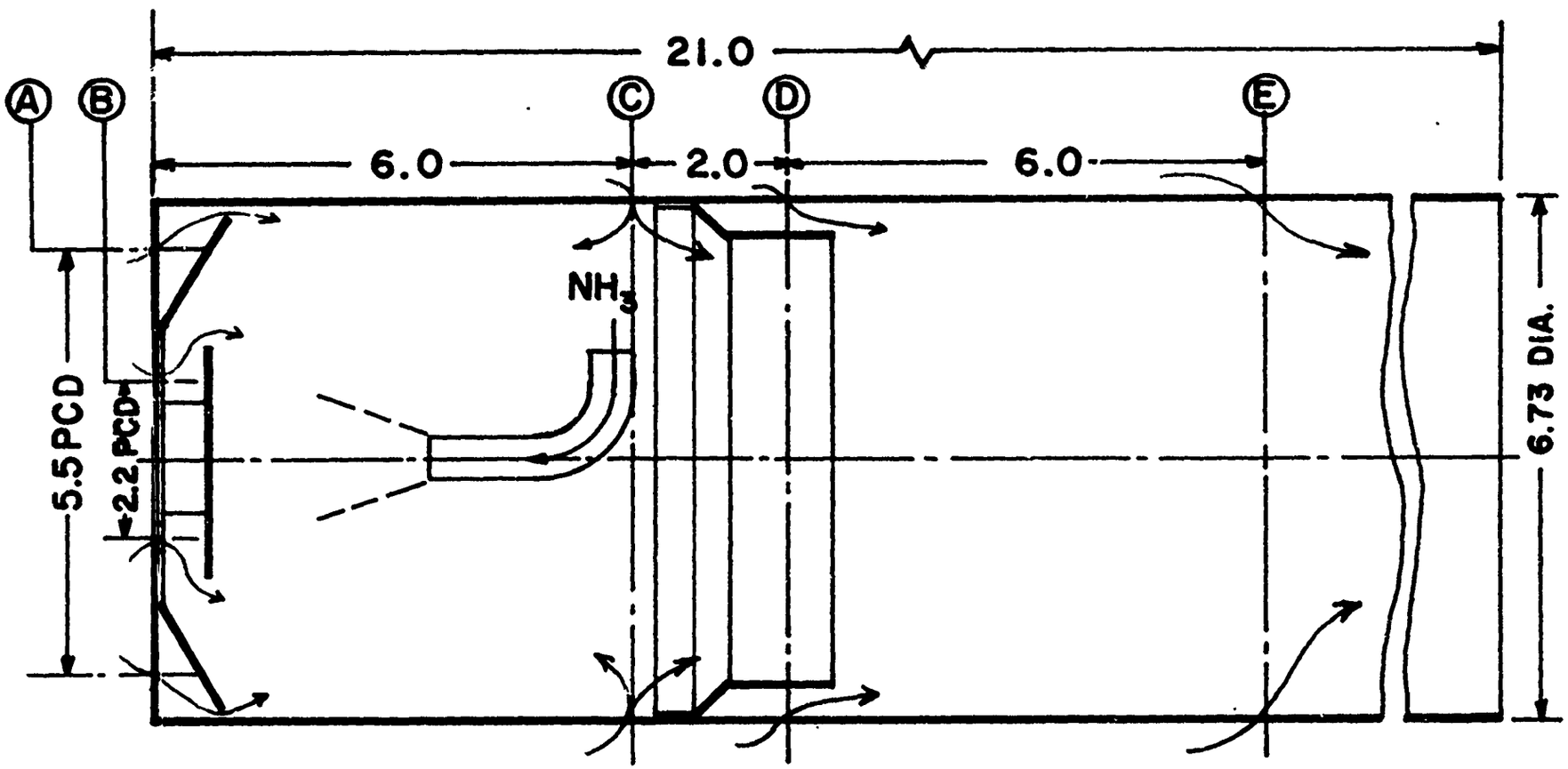

HOLE PATTERN		
LOCATION	NO	DIAM. (IN.)
A	24	5/16
B	8	5/16
C	8	9/32
D	24	9/32
E	12	11/16

Figure 1. Final Ammonia Vapor Combustor Design by Solar. O.D. = 6.75 in.

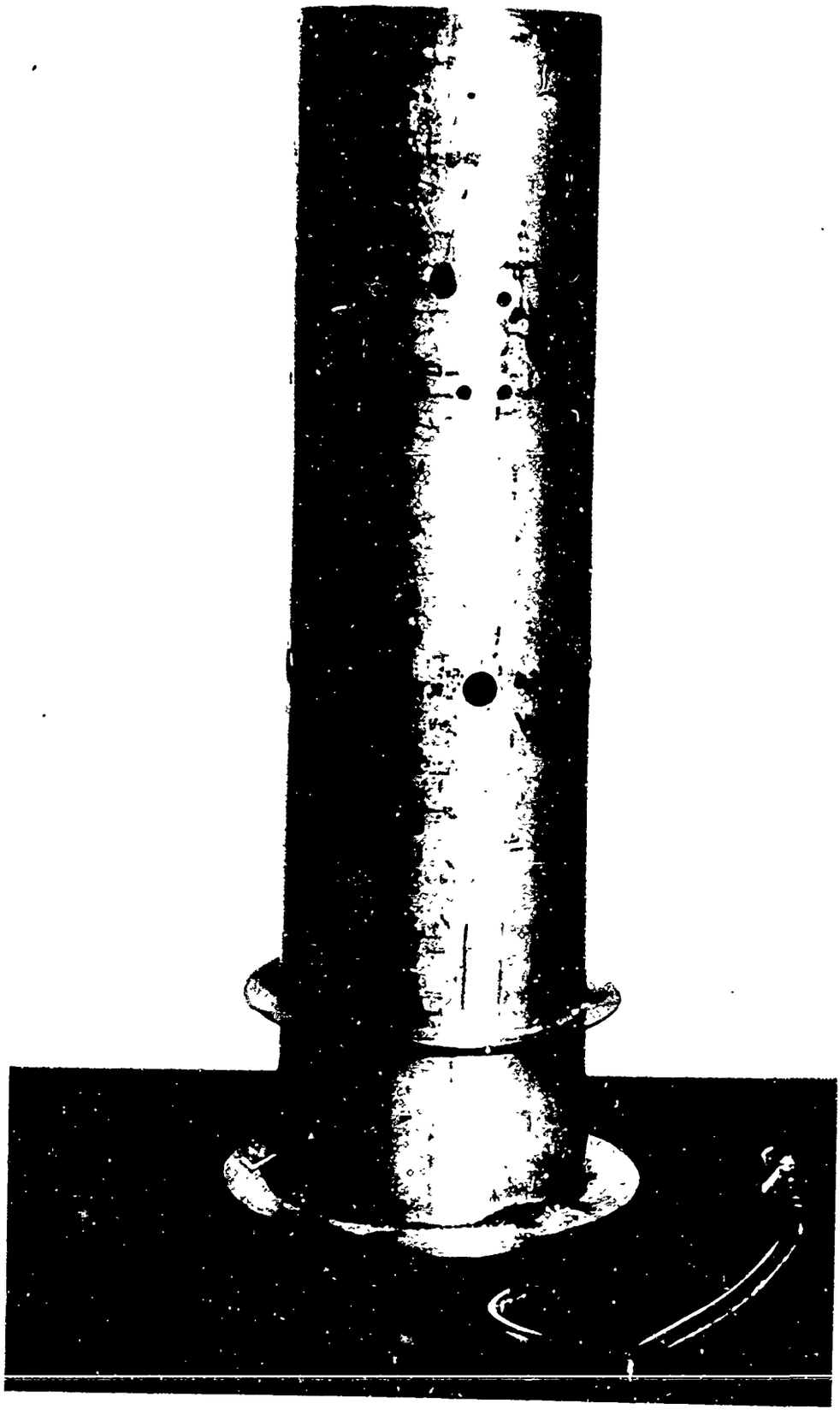

Figure 2a. 3/5-Scale model of Solar Combustor and fuel nozzle. O.D. = 4.04 in.

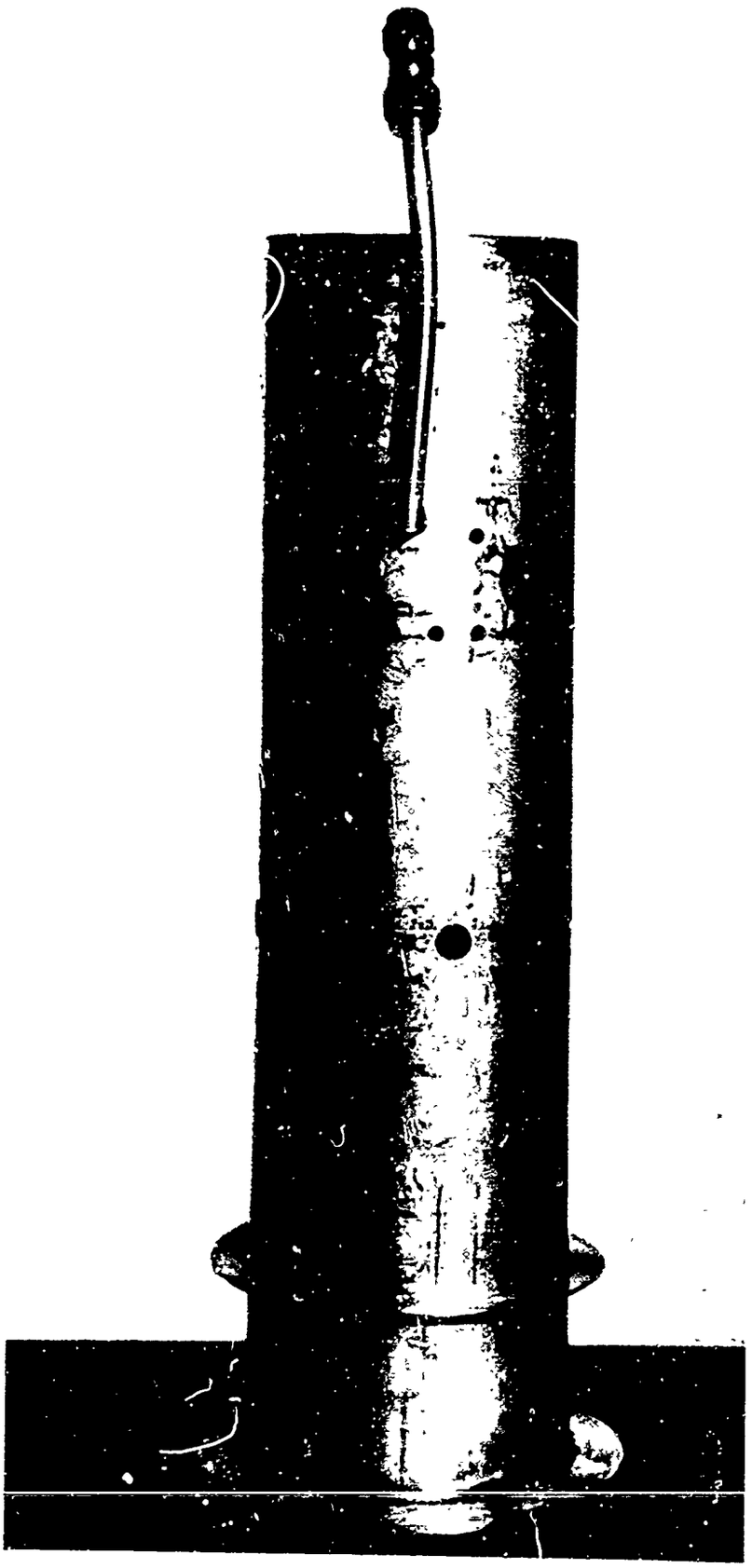

Figure 2b. 3/5-Scale model of Solar Combustor with fuel nozzle installed.

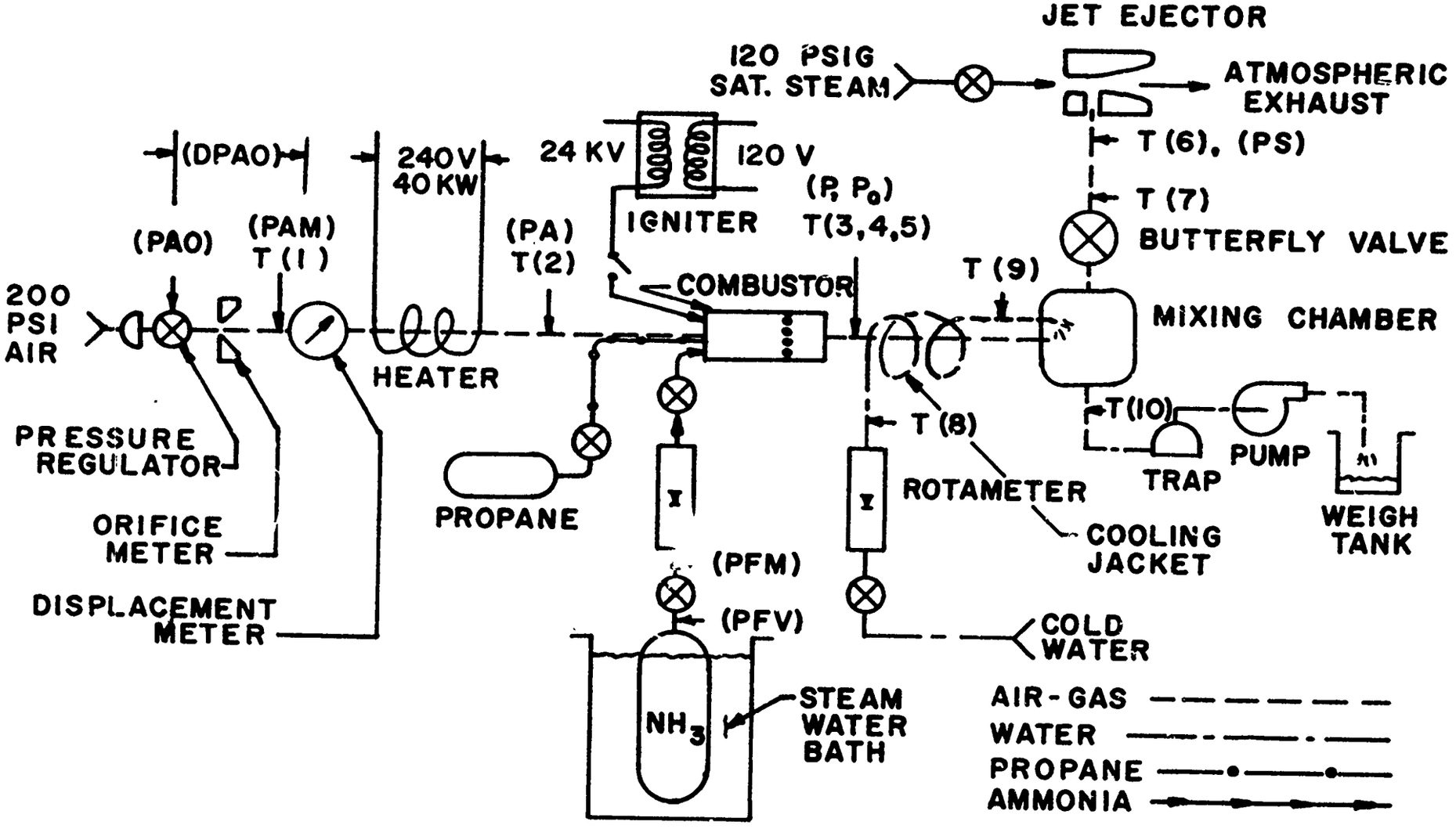

Figure 3. SCHEMATIC — COMBUSTOR INSTALLATION AND INSTRUMENTATION

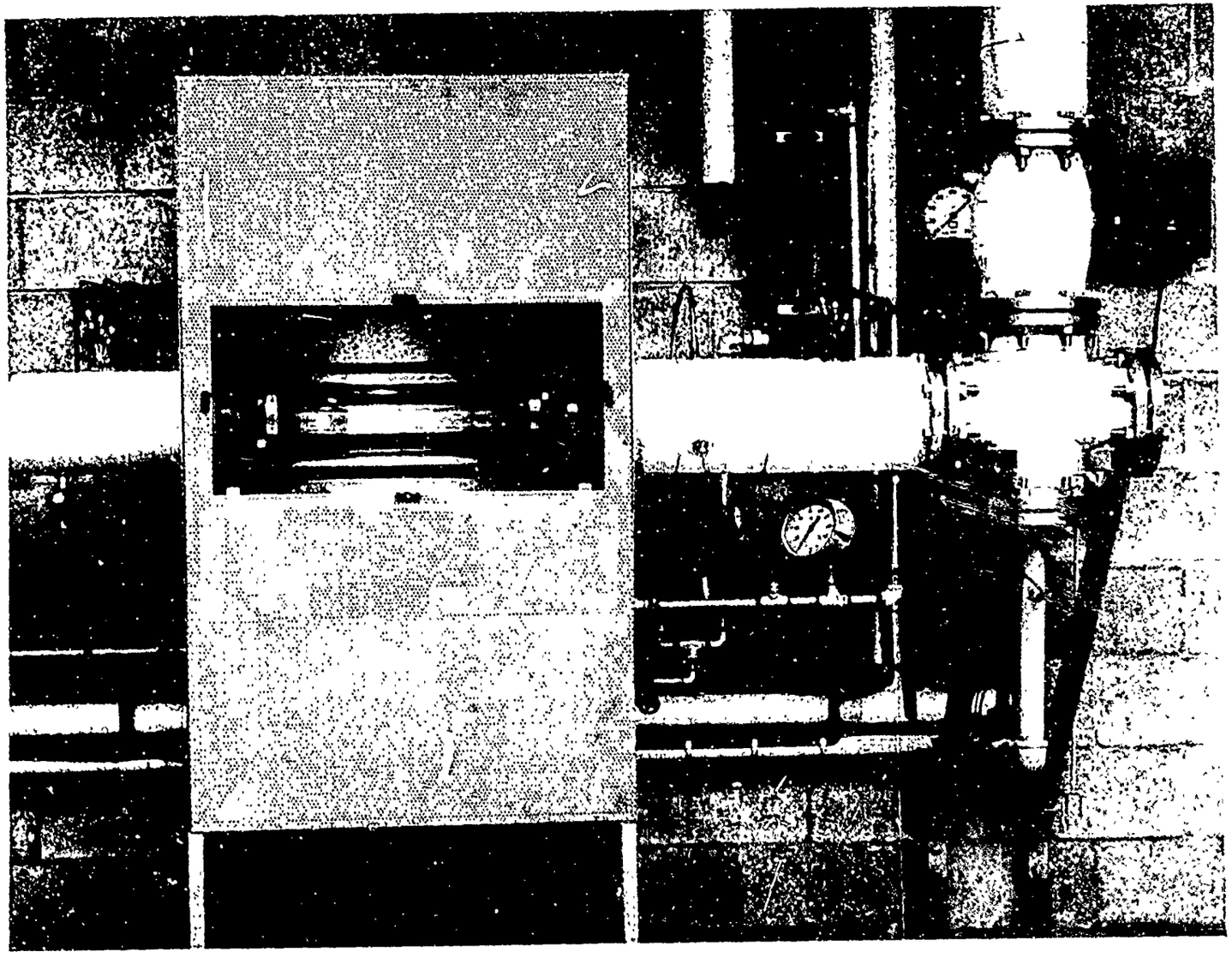

Figure 4. 5-Inch Combustor Housing.

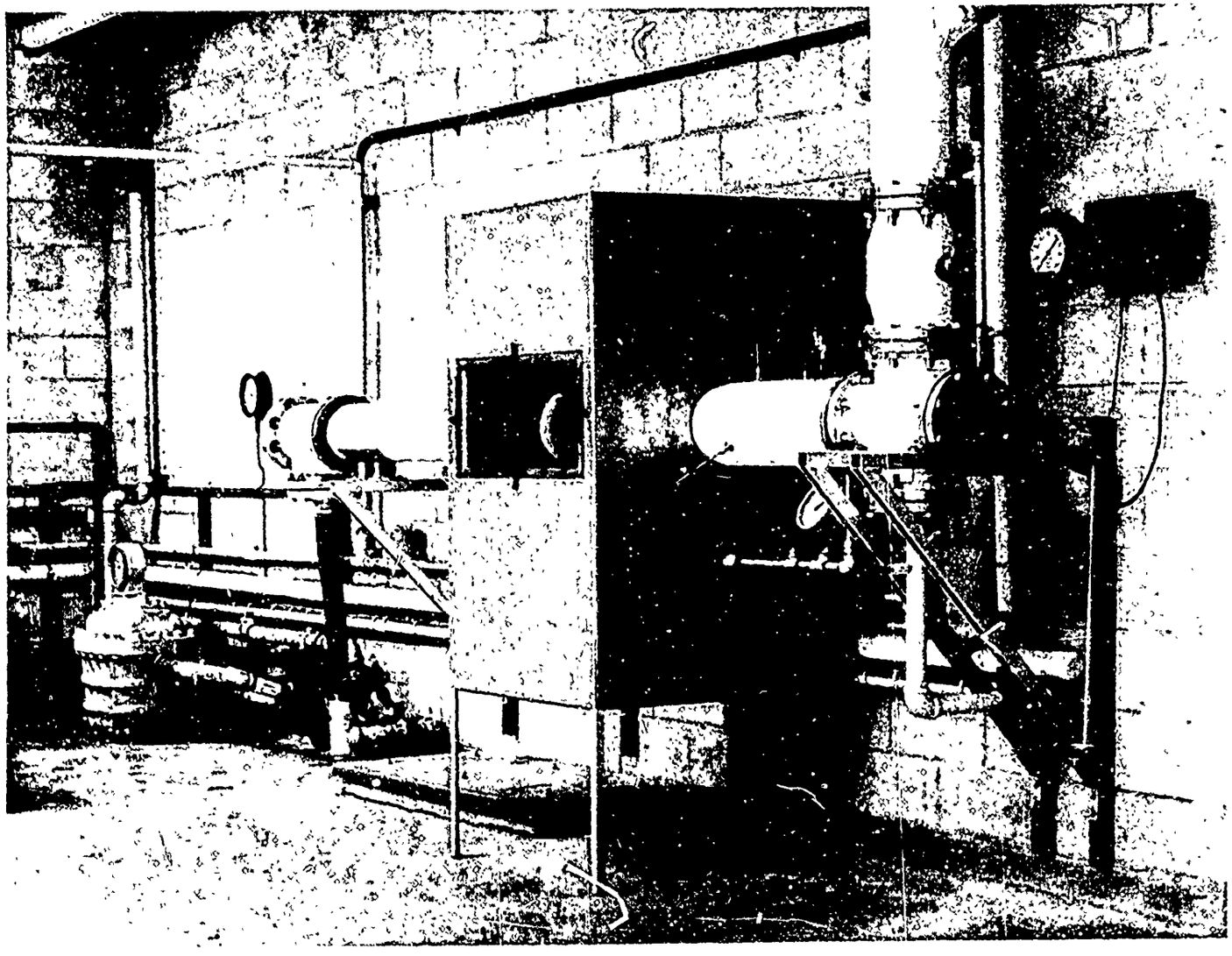

Figure 5. Oblique view of 5" combustor housing, air supply and metering section.

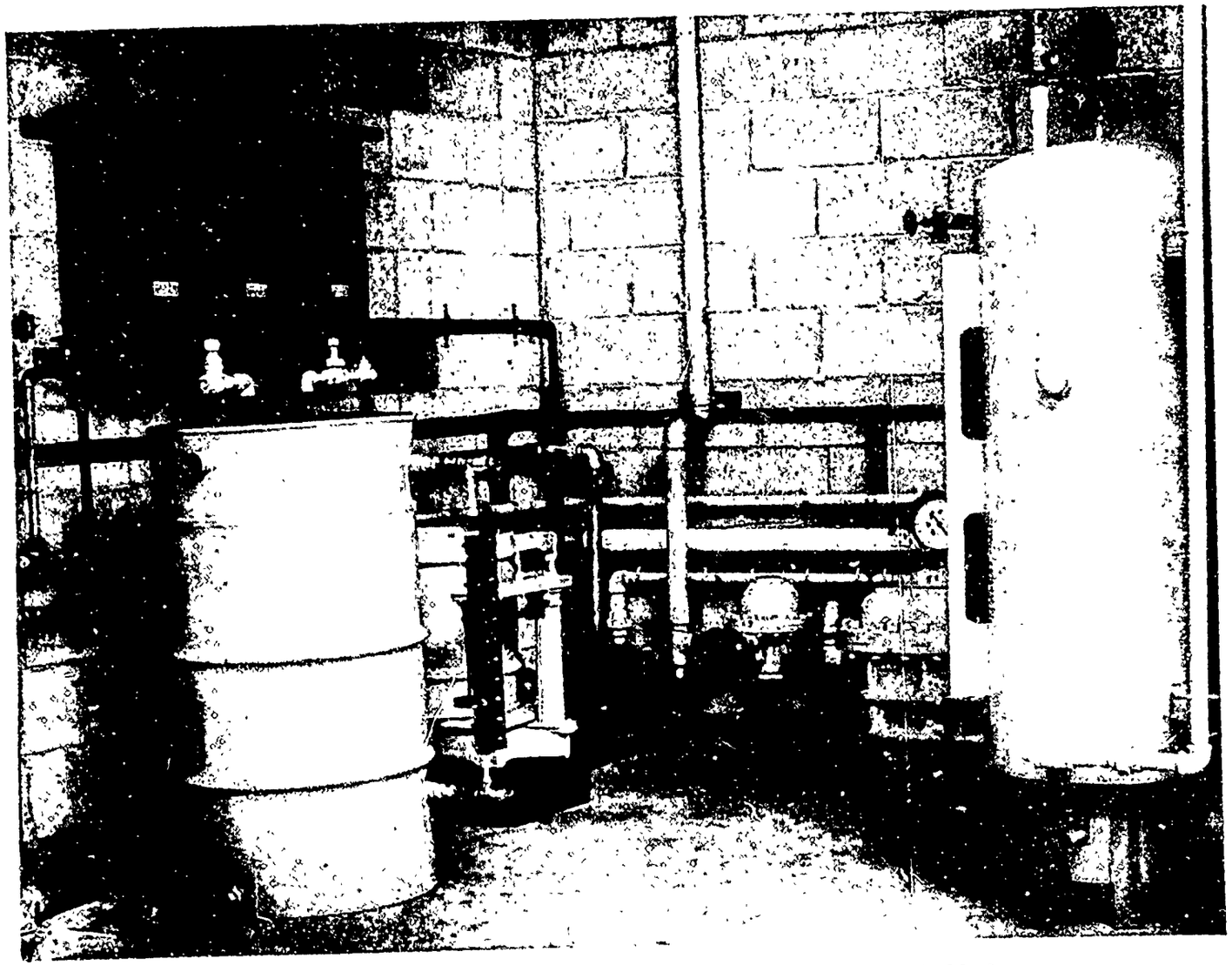

Figure 6. Ammonia vaporizer system, partially installed.

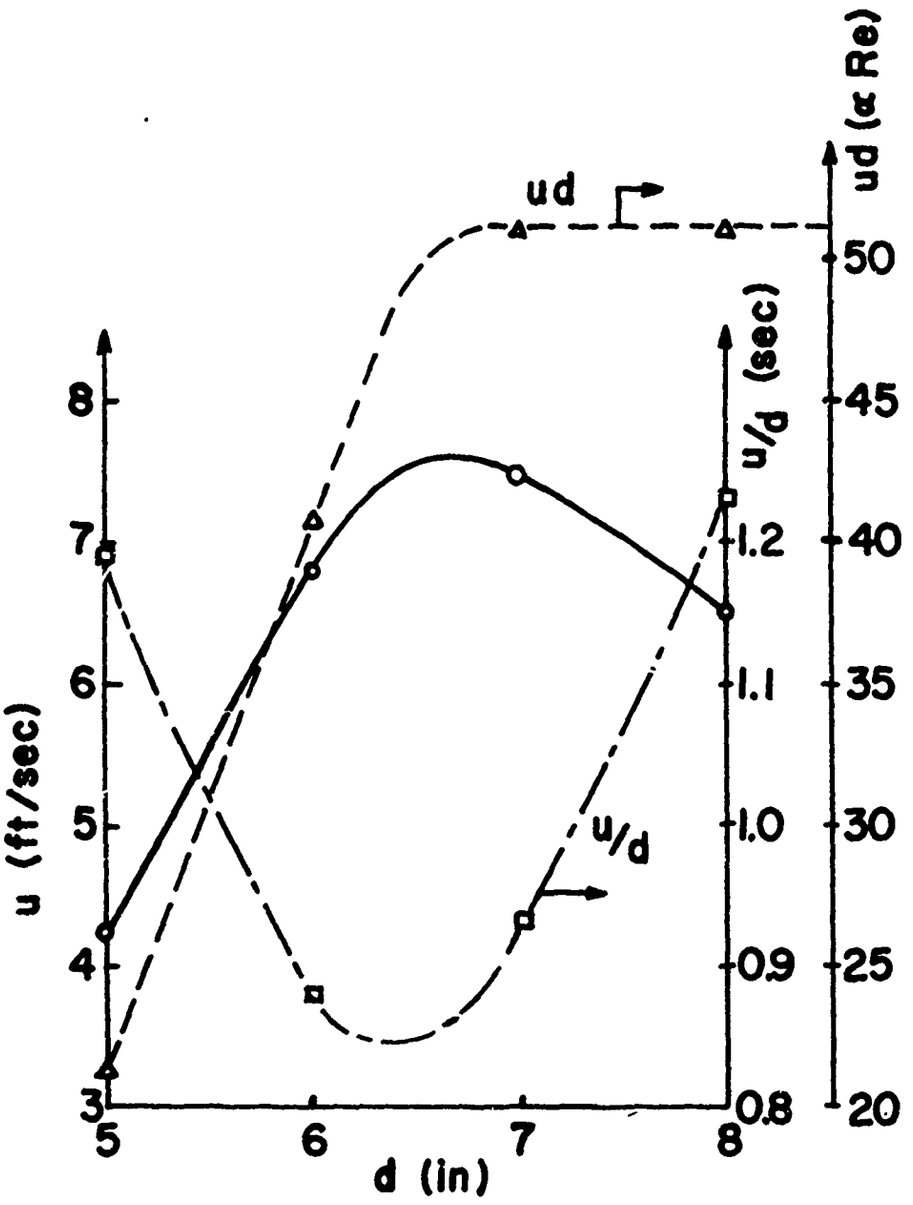

Figure 7. Maximum Blowout Velocity, Reynolds Number and Residence Time for Solar Scaling Combustors. T_{in} = 372 F, P_{in} = 26 psia.

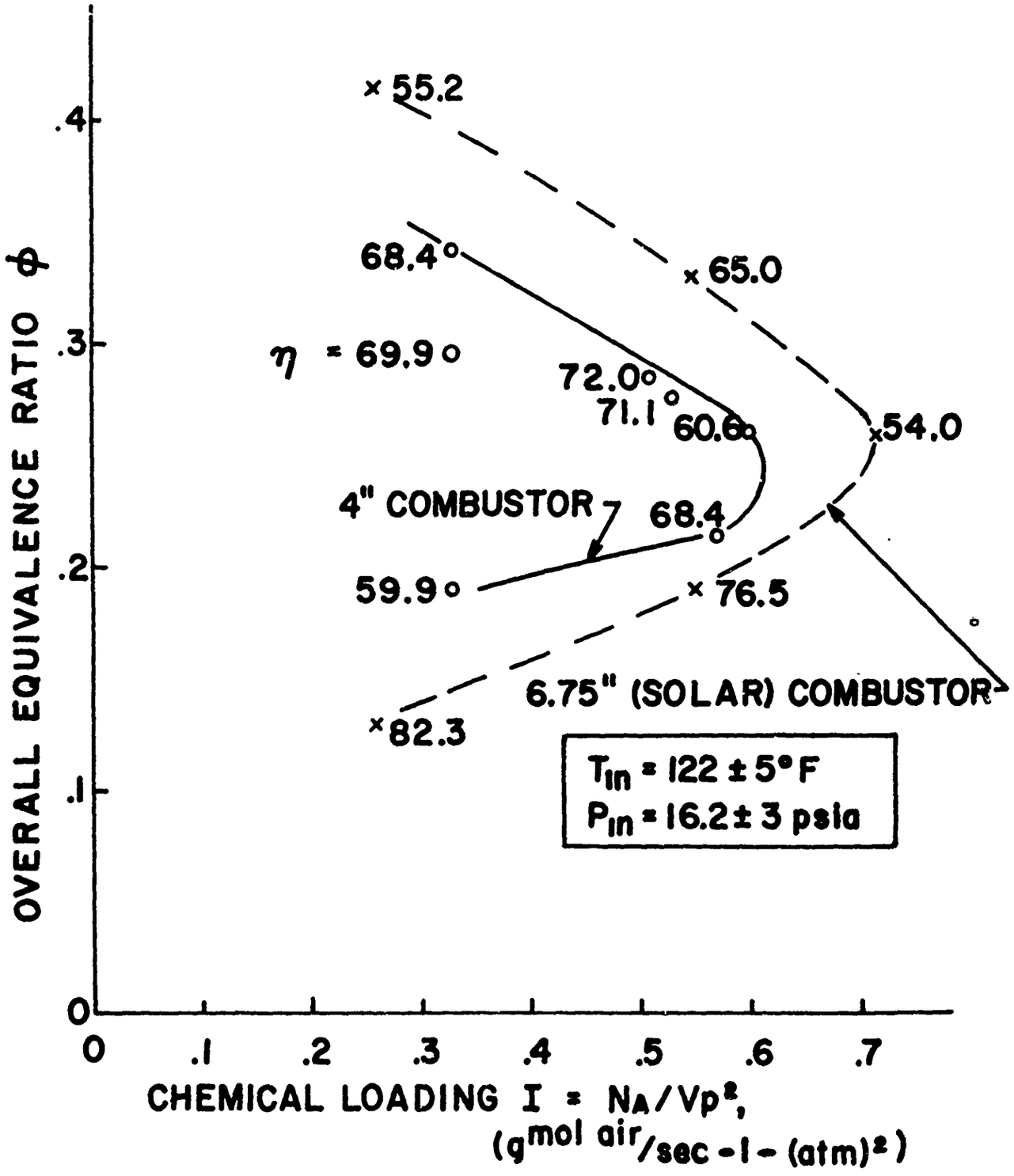

Figure 8. Overall Equivalence Ratio vs. Chemical Loading.
(Numbers by data points are combustion efficiencies.)

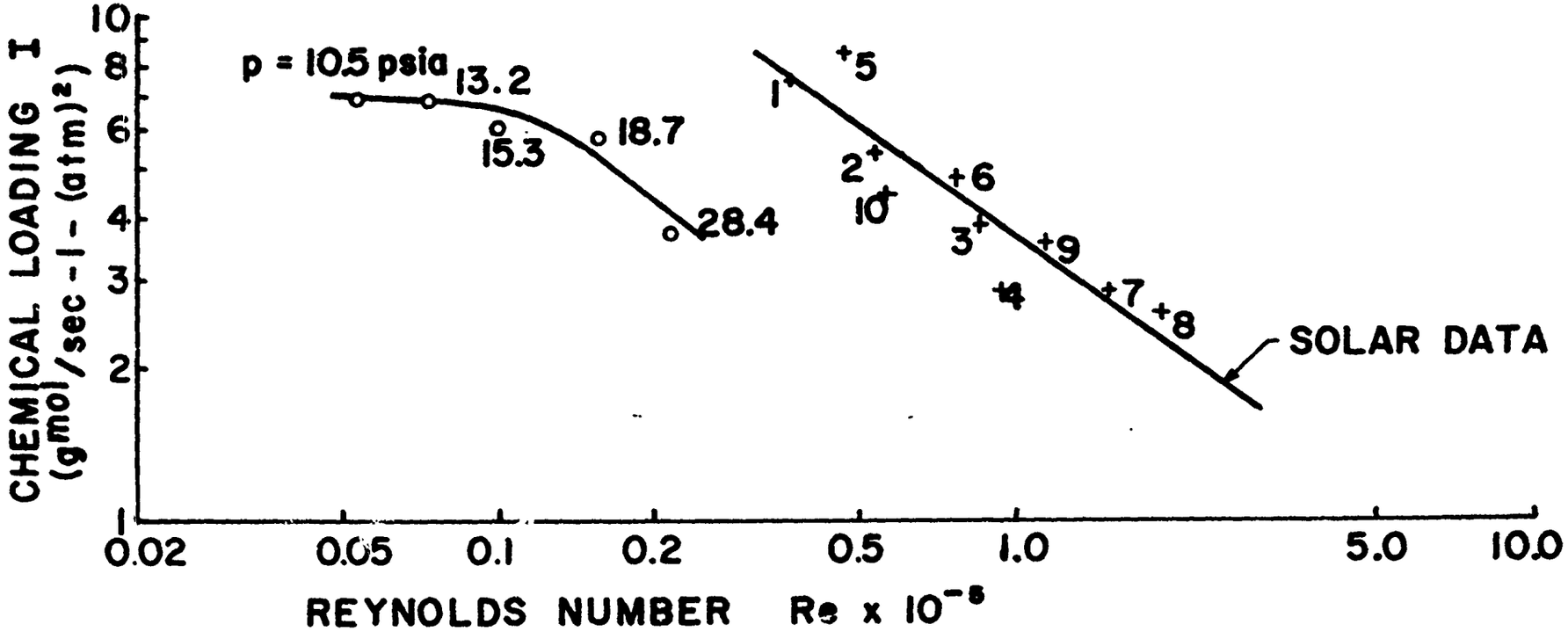

Figure 9. Chemical Loading vs. Reynolds Number at Maximum Blowout Velocity.
(Determination of effective reaction order.)

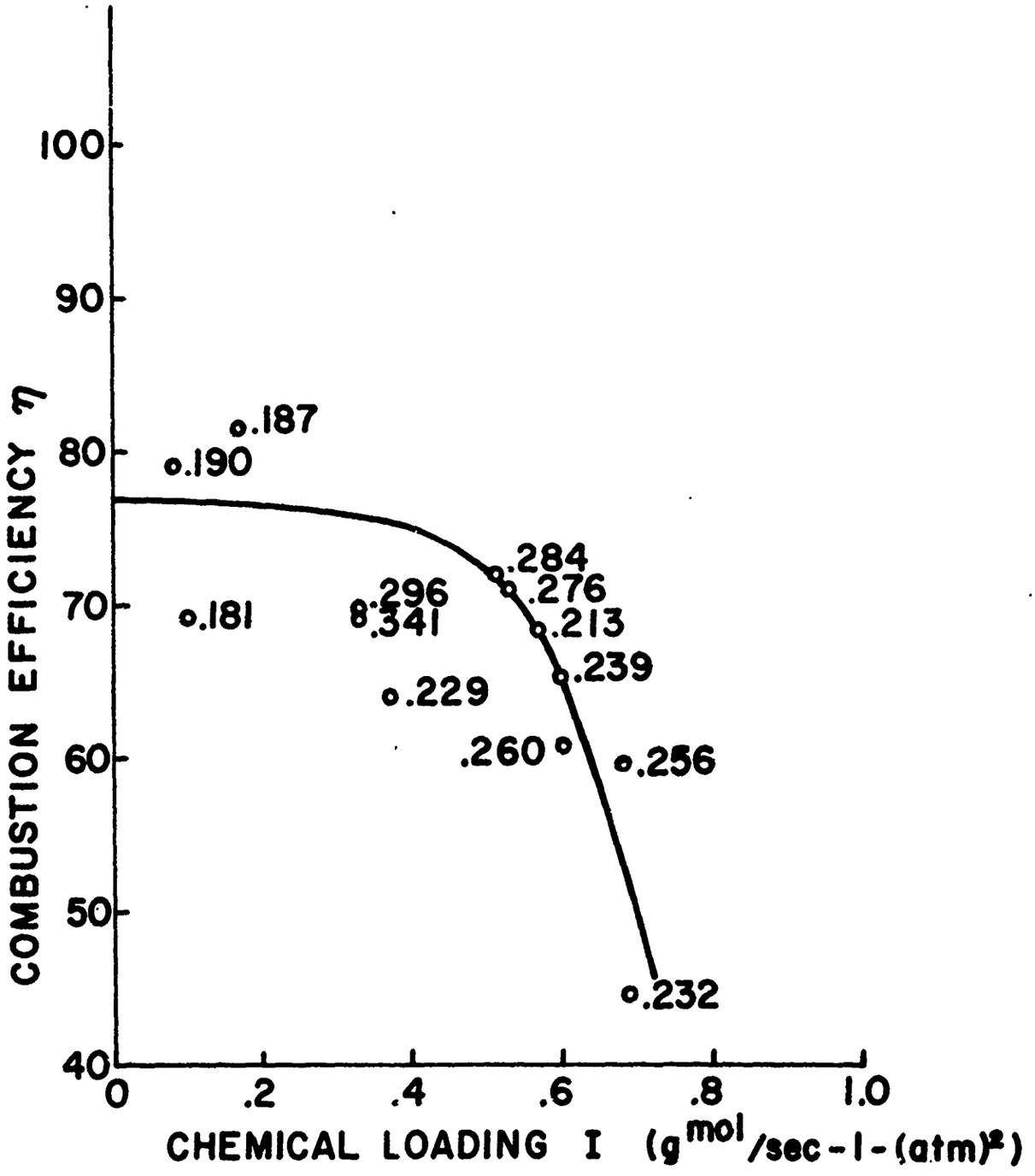

Figure 10. Chemical Loading vs. Combustion Efficiency.
(Numbers by data points are equivalence ratios.)

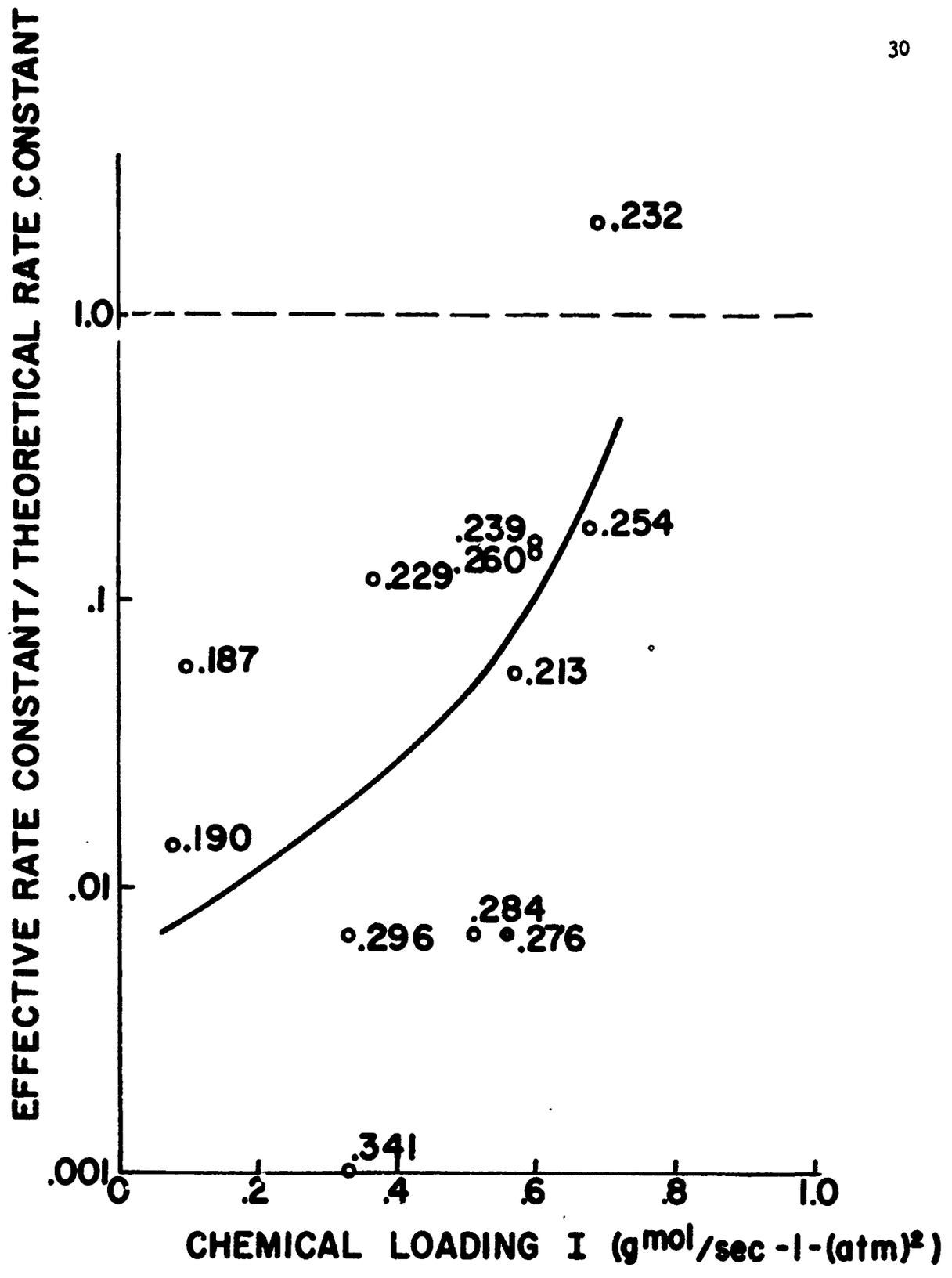

Figure 11. Ratio of Effective Rate Constant to Theoretical Rate Constant vs. Chemical Loading. (Numbers by data points are equivalence ratios.)